CARBON 54 (2013) 454–459

Available at www.sciencedirect.com

SciVerse ScienceDirect

journal homepage: www.elsevier.com/locate/carbon

Few layer graphene to reduce wear and friction on sliding steel surfaces

Diana Berman [a], *Ali Erdemir* [b], *Anirudha V. Sumant* [a,*]

[a] *Center for Nanoscale Materials, Argonne National Laboratory, 9700 S. Cass Ave., Argonne, IL 60439, United States*
[b] *Energy Systems Division, Argonne National Laboratory, 9700 S. Cass Ave., Argonne, IL 60439, United States*

ARTICLE INFO

Article history:
Received 21 August 2012
Accepted 30 November 2012
Available online 8 December 2012

ABSTRACT

We report that solution-processed graphene layers reduce friction and wear on sliding steel surfaces in air (relative humidity, 30%). In tests with sliding steel surfaces, small amounts of graphene-containing ethanol solution decreased wear by almost 4 orders of magnitude and friction coefficients by a factor of 6. A possible explanation for these results is that the graphene layers act as a two-dimensional nanomaterial and form a conformal protective coating on the sliding contact interfaces, and these factors facilitate shear and slow down the tribo-corrosion, thus drastically reducing the wear.

1. Introduction

Minimizing friction and wear-related mechanical failures remains one of the greatest challenges for today's moving mechanical assemblies, and the search for new materials, coatings, and lubricants that can potentially avoid such failures continues around the globe. Many studies have pointed out that the friction and wear mechanisms differ for different materials operating under different thermal, environmental, and tribological conditions [1]. Most traditional methods of controlling friction and wear involve the use of solid and liquid lubricants. However, the quest for finding the perfect lubricant, which not only provides the lowest friction and wear, but also free of harmful additives or chemicals [2], still continues. An exciting new material that has been investigated widely for its multitude of unusual physical, mechanical, and electrical properties is graphene, a crystallographically perfect film of graphitic carbon [3–5]. The tribological properties of graphene are relatively unexplored, and the few studies published in the open literature have mainly focused on the nano- and micro-scale aspects [6–8] in particular using the friction force microscopy technique [9,10]. Thus, very little information is available on the macro-scale tribological properties of graphene.

In one of the macro-scale tribological studies, Kandanur et al. have shown that graphene, when mixed with polymers, imparts excellent wear resistance to the resultant composite material [11]. Graphitic layers (which help in reducing friction and wear in artificial joints) have also been detected in metal-on-metal hip replacements [12]. Moreover, graphene platelets have been used as an oil additive for improved lubricity and wear resistance [13]. More importantly, graphene acts as an excellent corrosion protection layer on refined metals, such as copper and nickel [14,15], employed in reactive environments for many industrial applications. This protection, which is due to graphene's impermeability to gas molecules [16], is expected to work for steel interfaces studied in this paper. Graphene and other carbon-based nanomaterials are used to enhance protective properties of different lubricants [17–19]. Previous tribological studies using graphite flakes indicated formation of graphite scrolls at the tribological interface [20]. These scrolls are favorable for decreasing surface energy [21,22], and reducing friction in the sliding interfaces. All of these findings indicate that graphene has high potential as a self-lubricating material that will combat

* *Corresponding author.*
E-mail address: sumant@anl.gov (A.V. Sumant).
0008-6223/$ - see front matter
http://dx.doi.org/10.1016/j.carbon.2012.11.061

friction and wear-related energy and material losses in various dry and lubricated tribological applications.

In this paper, we propose that the anti-corrosion property of few layer graphene coupled with its lubricating nature would be beneficial in drastically reducing wear and friction in the case of the most commonly used tribo-pairs, in particular, steel against steel.

2. Experimental procedure

Tribological studies of steel flat samples against steel balls were performed in air (30% RH) at room temperature using a CSM tribometer with a ball-on-disk contact geometry. The stainless steel flat samples (440C grade) were initially cleaned by sonication in acetone and then in isopropanol alcohol to remove any organic contaminants that may have been left from the machining and polishing operations performed during sample preparation. The counterpart was stainless steel ball (440C grade) of 9.5 mm diameter with the rms roughness measured by the 3D profilometer R_q = 15 nm. The normal load during the tribotests was 2 N at a speed of 60 rpm (or 9 cm/s), and the radius of the wear track was 15 mm. The sliding test durations were 2000 cycles or 190 m.

Solution-processed graphene (SPG) was prepared by chemical exfoliation of highly oriented pyrolytic graphite (HOPG) and was then suspended in ethanol (Graphene Supermarket Inc.). The weight concentration of graphene was 1 mg/L. Before the tribological tests, graphene-containing ethanol solution was spread on the highly polished surfaces (rms roughness measured by the 3D profilometer R_q = 20 nm) of the stainless steel plates and evaporated in a dry nitrogen environment to prevent graphene oxidation. Formation of few-layer graphene (2–3 layers) on the steel surface was confirmed by examination with an Invia confocal Raman microscope using red laser light (λ = 633 nm). The imaging of the wear scars was performed with an Olympus UC30 microscope. The wear rates on the ball and the flat sides were determined with a 3D non-contact MicroXam profilometer.

To estimate the wear rate after the tests, we calculated the wear volume of the ball side as follows:

$$V = \left(\frac{\pi h}{6}\right)\left(\frac{3d^2}{4} + h^2\right) \quad (1)$$

where d is the wear scar diameter, r is the radius of the ball, and

$$h = r - \sqrt{r^2 - \frac{d^2}{4}} \quad (2)$$

3. Results and discussion

To study the effect of graphene on the friction and wear of sliding steel test pairs in a humid air environment, we performed three model experiments: (1) steel against steel, (2) steel against SPG on steel submerged in liquid SPG, and (3) steel against SPG on steel with an intermittent supply of SPG drops every 400 cycles. The occasional supply of SPG was necessary to ensure that graphene was present in the wear track throughout the test period. Fig. 1 presents the coefficients of friction for all three cases. The coefficient of friction (COF) for bare steel interfaces was initially low, then increased rapidly with the removal of the surface contaminants and/or a natural oxide layer from the surface, and finally reached a value of about 0.9 for the reminder of the test. The COF for the test performed in liquid SPG solution after the ethanol treatment was reduced to 0.2. This COF reduction is thought to be due to the combined lubrication effect of ethanol and graphene flakes. However, tests performed with pure ethanol lubricant (results are also shown in Fig. 1) showed a higher COF (0.4) and caused high wear, suggesting that graphene is most likely the reason for the friction reduction. As it can be seen from the Fig. 1, after 700 cycles the variations in the coefficient of friction for the steel interfaces in ethanol increase as well as the average value of the COF increases. This can be attributed to the influence of the steel corrosion effect, confirmed by the Raman signature (not shown here) indicating well pronounced peak at 700 cm^{-1} attributed to iron oxide as well as high wear summarized in Table 1. For the last data set, SPG was supplied to the wear track periodically in drops (2–3 drops or 0.1–0.15 mL of solution) every 400 ± 100 cycles. As shown in Fig. 1, this test

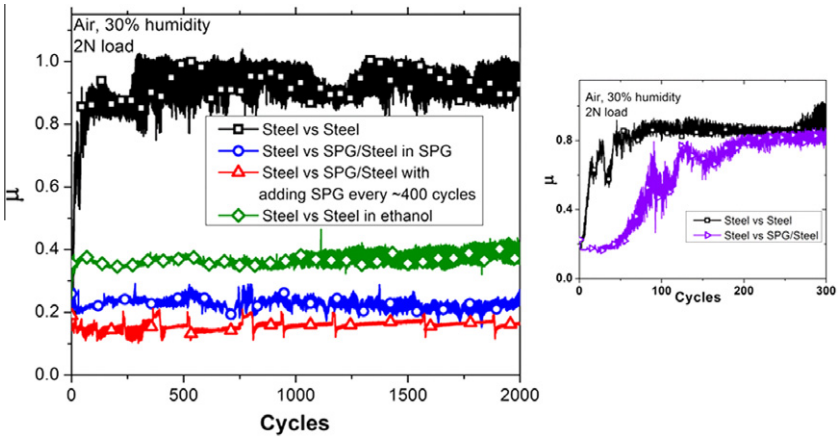

Fig. 1 – Coefficients of friction (μ) for self-mated steel test pair in humid air without SPG, without SPG in ethanol, with SPG in ethanol solution, and with intermittent supply of SPG. Moreover, the COF results for steel with and without initial SPG layer are provided in the inset to show necessity of additional graphene supply during the run.

Table 1 – Ball wear calculations and COF measurements for the tests in air.

Test Conditions	Calculated Wear Volume (2000 cycles)	Wear Rate (Wear/(load·distance)	Established Measured COF
Without SPG	6.8×10^{-3} mm^3	179.9×10^{-7} mm^3/N m	0.91
In ethanol	7.2×10^{-4} mm^3	19.1×10^{-7} mm^3/N m	0.38
In liquid SPG	5.0×10^{-5} mm^3	1.3×10^{-7} mm^3/N m	0.23
Adding drops of SPG every 400 cycles	1.1×10^{-6} mm^3	0.03×10^{-7} mm^3/N m	0.15

reduced the COF to around 0.15. This friction reduction can be attributed to the continuous supply of graphene layers into the sliding contact interface. The periodicity of 400 cycles (or every 6–7 min) is long enough to evaporate the ethanol from the steel surface (about 20–30 cycles are necessary for complete evaporation), thus eliminating the alcohol's contribution or effect, but leaving behind the graphitic layer within the wear track. Moreover, the fairly stable frictional behavior attained by adding drops of SPG into the sliding interface indicates that the low friction values can be preserved for quite a long time. The required period of dropping the SPG solution was noticed to prolong with time which indicates formation of the stable tribolayer. The procedure of adding the drops of solution showed to be effective even up to 4000 cycles (the test was stopped after 4000 cycles) without any change in friction performance. Importance of replenishing the graphene layer can be seen from the inset of the Fig. 1. In this case the initial graphene layer during sliding was removed quickly out of the wear track and resulted in high COF. The short lifetime of the initial deposited layer is attributed to low concentration of graphene.

The above results clearly confirm the friction-reducing effect of SPG. In the following, we will discuss its impact on wear, specifically, the wear rates on the ball and flat sides with and without SPG on sliding surfaces.

Fig. 2 shows optical micrographs of the wear scars and tracks on the ball and flat sides, respectively, after the tests. The difference in the wear scar diameter and the wear track

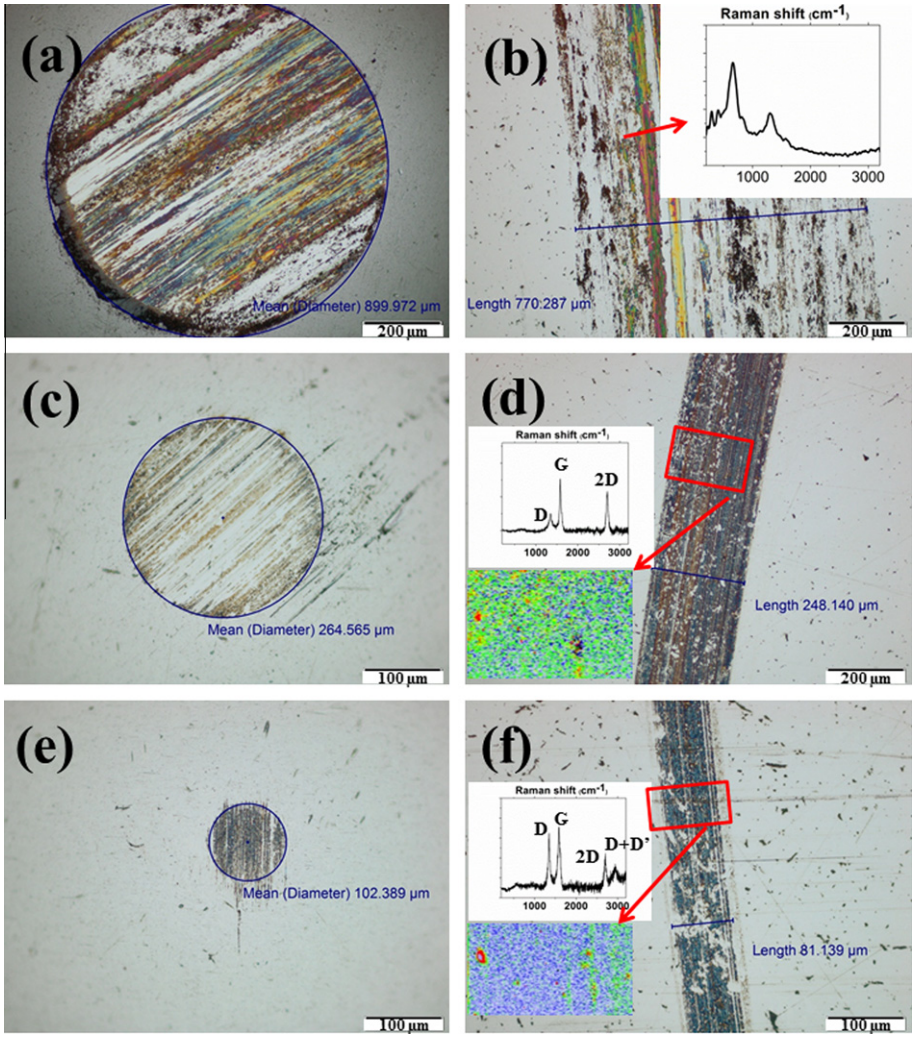

Fig. 2 – Optical micrographs of wear scars and tracks on the ball and flats, respectively, after tests without SPG solution (a and b), with SPG solution (c and d), and with drip feeding of SPG every 400 cycles (e and f).

width is attributed to the fact that the wear track width varies along the wear track thus resulting in smaller average width of the wear scar. Also, the ball suffers higher Hertz pressure effects on the sides of the wear scar than the flat side, thus resulting in wider wear scar width.

When tested in open air, the steel ball and flat suffer severe wear damage, as shown in Fig. 2a and b. The wear damage decreases when SPG is added to the wear track (Fig. 2c–f). Raman spectra of the wear tracks after the tribotests with and without SPG are also presented as insets on Fig. 2b, d, and f. Raman mapping of these tracks (inset below the spectra) shows the concentration and intensity of the 2D peak of graphene (at ~2700 cm^{-1}, red color corresponds to the highest intensity, blue to the lowest when no peak is present) after the run. For the test in the liquid SPG solution, after the test was finished and the solution dried off, the 2D peak of graphene was detected everywhere on the wear scar due to unmodified graphene in the solution (Fig. 2d). For the case of adding drops of SPG to the sliding surfaces, the graphene had become defected and disordered during the sliding tests, and this process resulted in a significant reduction of 2D peak intensity in the wear scar with better signal around the wear scar edges, which are less affected by the wear process (Fig. 2f). The Raman spectrum of the wear scar edges shows disordered graphene, as evidenced from the D peak intensity (at ~1350 cm^{-1}, I_D/I_G increased from 0.3 for liquid SPG solution to almost 1 for adding SPG drops) (Fig. 2f). For the drip SPG run, another graphene Raman peak, D + D' (at ~2940 cm^{-1}), is activated by defects in the graphene layers. This finding supports the fact that sliding interfaces produce defected graphene.

Previous studies [23–30] used Raman spectra for corrosion investigation of stainless steel and showed the characteristic peaks of iron oxides at ~700 cm^{-1} and below. The Raman signatures of the wear tracks with SPG (Fig. 2f) show a very weak signal for iron oxides (below 700 cm^{-1}) in contrast to the bare steel run (Fig. 2b), suggesting that graphene reduces oxidation-induced corrosion of the steel.

Fig. 3 presents 3D profilometer images and height profiles of the same wear tracks shown in Fig. 2. The high wear occurs mostly for the bare steel interfaces when no protective layer exists (width of the scar is 770 μm). For the liquid SPG solution run (Fig. 3b), the wear scar width is 3 times smaller (~250 μm) than that of the bare steel run (Fig. 3a). Line profile measurements indicate formation of a graphene protection layer (as confirmed by Raman spectroscopy), shown in Fig. 2d. However, due to the presence of liquid in the wear track, the capillary forces at the interface do not allow formation of a uniform protection layer, and the graphene flakes are continuously pushed away on the side of the wear

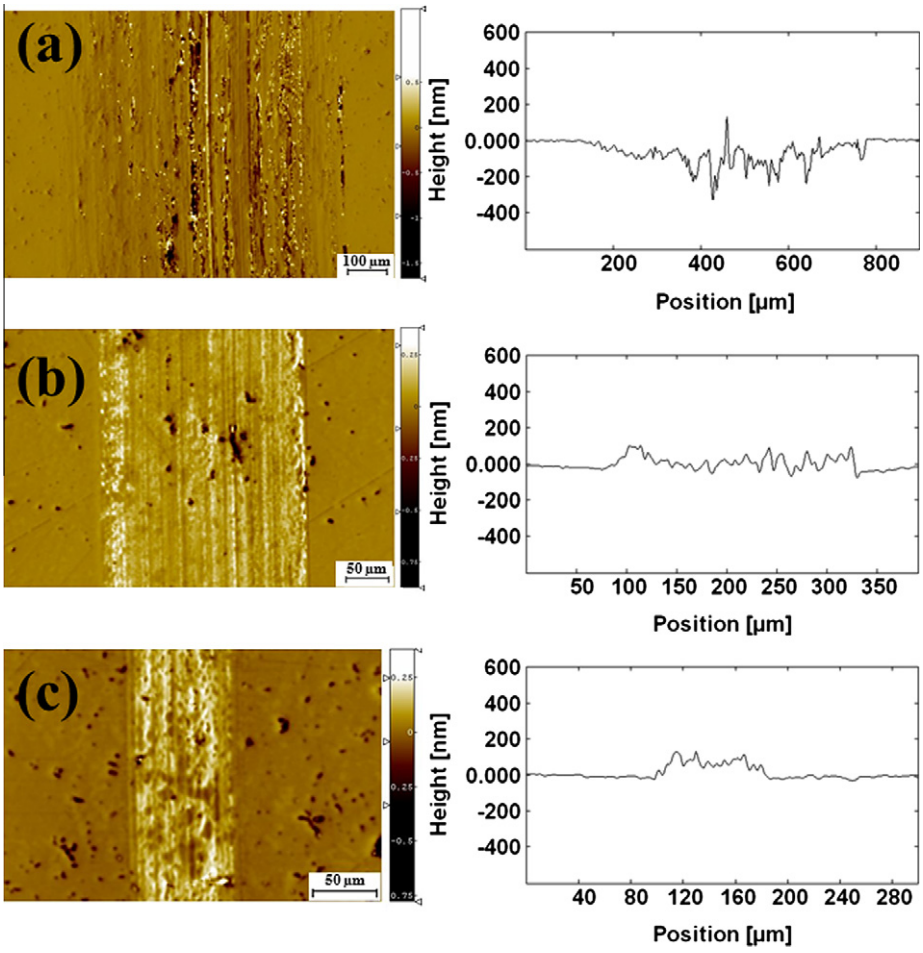

Fig. 3 – Height profile measurements of the wear tracks for (a) steel against steel, (b) steel against SPG/steel in liquid SPG, and (c) steel against SPG/steel with SPG added every 400 cycles.

track during each wear cycle. Therefore, the density of graphene is too low to form a uniform protection layer within the wear track. For the drip SPG run, the wear track width was 10 times smaller (~80 μm) than that of bare steel. This finding indicates that graphene forms a uniform protection layer and thus plays a major role in reducing wear and friction at the tribological interface. The corresponding line profile of the wear track in this case (Fig. 3c) indicates formation of a protective layer on the steel. 3D profilometer imaging of the ball wear for this test indicated that the wear occurs at the initial stage, with subsequent formation of the protective layer.

The measured established COFs (averaged over last 500 cycles) and the wear results for the ball sides calculated using Eq. (1)are summarized in Table 1. The ball wear diameters, which were measured with an Olympus UC30 Microscope, are presented in Fig. 2.

The results in Table 1show that wear is reduced by 2–3 orders magnitude due to graphene in the wear track. The wear on the flat side in the case of SPG-coated steel is almost impossible to measure, indicating the major contribution of graphene in reducing wear and friction. Adding SPG drops is the more effective method of friction and wear reduction, which we attribute to the drops supplying renewable graphene layers with a high concentration in the wear track. The tribotest in liquid SPG solution, by contrast, is limited in the initial amount of graphene.

We show that the graphene-based lubricant studied here offers a significant benefit in terms of reducing toxic waste to the environment and provides a new pathway for reducing wear and friction that could be exploited further for many industrial applications involving sliding and rotational contacts.

4. Conclusion

A series of experiments was conducted to test the wear and friction behavior of self-mated steel tribo-pairs in humid air with SPG supplied at the tribological interface. Wear of the self-mated steel surfaces was substantially reduced (3–4 orders of magnitude) with corresponding reduction in friction (6×) by the presence of graphene at the tribological interface. Characterization of the wear track by Raman imaging and spectroscopy revealed suppression of the iron oxide peak and the presence of graphene. These results indicate a passivation effect due to the graphene layers, which not only helped in reducing the tribo-corrosion and thus resulted in low wear, but also provided easy shearing and thus resulted in reduced friction. We conclude that graphene constitutes a new class of lubricant for steel surfaces and possibly other metal surfaces that is corrosion resistant, less toxic, and easy to apply.

Acknowledgments

Use of the Center for Nanoscale Materials was supported by the U.S. Department of Energy, Office of Science, Office of Basic Energy Sciences, under Contract No. DE-AC02-06CH11357.

REFERENCES

[1] Ludema KC. Friction, wear, lubrication: a textbook in tribology. Florida: CRC Press, Inc.; 1993. p. 69–155.
[2] Khorramian BA, Iyer GR, Kodali S, Natarajan P, Tupil R. Review of antiwear additives for crankcase oils. Wear 1993;169:87–95.
[3] Peng B, Locascio M, Zapol P, Li S, Mielke SL, Schatz GC, et al. Measurements of near-ultimate strength for multiwalled carbon nanotubes and irradiation-induced crosslinking improvements. Nat Nanotechnol 2008;3:626–31.
[4] Schwarz UD, Zworner O, Koster P, Wiesendanger R. Quantitative analysis of the frictional properties of solid materials at low loads. Phys Rev B 1997;56:6987–96.
[5] Yu M-F, Lourie O, Dyer MJ, Moloni K, Kell TF, Ruoff RS. Strength and breaking mechanism of multiwalled carbon nanotubes under tensile load. Science 2000;287(5453):637–40.
[6] Lee CG, Wei XD, Kysar JW, Hone J. Measurement of the elastic properties and intrinsic strength of monolayer graphene. Science 2008;321:385–8.
[7] Gómez-Navarro C, Burghard M, Kern K. Elastic properties of chemically derived single graphene sheets. Nano Lett 2008;8(7):2045–9.
[8] Gao YW, Hao P. Mechanical properties of monolayer graphene under tensile and compressive loading. Physica E 2009;41(8):1561–6.
[9] Lee C, Wei X, Li Q, Carpick R, Kysar JW, Hone J. Elastic and frictional properties of graphene. Phys Status Solidi B 2009;246(11–12):2562–7.
[10] Deng Z, Smolyanitsky A, Li Q, Feng X-Q, Cannara RJ. Adhesion-dependent negative friction coefficient on chemically modified graphite at the nanoscale. Nat Mater 2012. http://dx.doi.org/10.1038/nmat3452.
[11] Kandanur SS, Rafiee MA, Yavari F, Schrameyer M, Yu ZZ, Blanchet TA, et al. Suppression of wear in graphene polymer composites. Carbon 2011. http://dx.doi.org/10.1016/j.carbon.2011.10.038.
[12] Liao Y, Pourzal R, Wimmer MA, Jacobs JJ, Fischer A, Marks LD. Graphitic tribological layers in metal-on-metal hip replacements. Science 2011;334:1687–90.
[13] Lin J, Wang L, Chen G. Modification of graphene platelets and their tribological properties as a lubricant additive. Tribol Lett 2011;41:209–15.
[14] Prasai D, Tuberquia JC, Harl RR, Jennings GK, Bolotin KI. Graphene: corrosion-inhibiting coating. ACS Nano 2012;6(2):1102–8.
[15] Chen S, Brown L, Levendorf M, Cai W, Ju SY, Edgeworth J, et al. Oxidation resistance of graphene coated Cu and Cu/Ni alloy. ACS Nano 2011;5:1321–7.
[16] Bunch JS, Verbridge SS, Alden JS, van der Zande AM, Parpia JM, Craighead HG, et al. Impermeable atomic membranes from graphene sheets. Nano Lett 2008;8:2458–62.
[17] Choudhary S, Mungse HP, Khatri OP. Dispersion of alkylated graphene in organic solvents and its potential for lubrication applications. J Mater Chem 2012;22:21032–9.
[18] Huanga HD, Tua JP, Ganb LP, Li CZ. An investigation on tribological properties of graphite nanosheets as oil additive. Wear 2006;261:140–4.
[19] Gupta BK, Bhushan B. Fullerence particles as an additive to liquid lubricants and greases for low friction and wear. Lubr Eng 1994;50:524–8.
[20] Spreadborough J. The frictional behavior of graphite. Wear 1962;5:18–30.
[21] Shioyama H, Akira T. A new route to carbon nanotubes. Carbon 2003;41(1):179–81.
[22] Li JL, Peng QS, Bai GZ, Jiang W. Carbon scrolls produced by high energy ball milling of graphite. Carbon 2005;43:2817–33.

[23] Hanesch M. Raman spectroscopy of iron oxides and (oxy)hydroxides at low laser power and possible applications in environmental magnetic studies. Geophys J Int 2009;177:941–8.
[24] Maslar JE, Hurst WS, Bowers WJ, Hendricks JH. In situ Raman spectroscopic investigation of stainless steel hydrothermal corrosion. Corrosion 2002;58:739–47.
[25] Boucherit N, Hugot-Le Goff A, Joiret S. Influence of Ni, Mo, and Cr on pitting corrosion of steels studied by Raman spectroscopy. Corros NACE 1992;48:569–79.
[26] Boucherit N, Hugot-Le Goff A, Joiret S. In situ Raman identification of stainless steels pitting corrosion films. Mater Sci Forum 1992;111–112:580–8.
[27] Ferreira MGS, Silva TME, Catarino A, Pankuch M, Melendres CA. Electrochemical and laser Raman spectroscopy studies of stainless steel in 0.15 M sodium chloride solution. J Electrochem Soc 1992;139:3146–51.
[28] Oblonsky LJ, Devine TM. Surface enhanced Raman spectroscopic study of the passive films formed in borate buffer on iron, nickel, chromium and stainless steel. Corros Sci 1995;37:17–41.
[29] Thanos ICG. Electrochemical reduction of thermally prepared oxides of iron and iron–chromium alloys studied by in situ Raman spectroscopy. Electrochim Acta 1986;31:1585–95.
[30] Thierry D, Persson D, Leygraf C, Delichère D, Joiret S, Pallotta C, et al. In-situ Raman spectroscopy combined with x-ray photoelectron spectroscopy and nuclear microanalysis for studies of anodic corrosion film formation on Fe–Cr single crystals. J Electrochem Soc 1988;135:305–10.